

Pharmacokinetic Study of Taxol-Loaded Poly(lactic-co-glycolic acid) Microspheres Containing Isopropyl Myristate after Targeted Delivery to the Lung in Mice

Hitoshi SATO,^a Ya Min WANG,^b Isao ADACHI,^a and Isamu HORIKOSHI^{*,a}

Department of Hospital Pharmacy, Toyama Medical and Pharmaceutical University,^a 2630 Sugitani, Toyama 930-01, Japan and Beijing Pharmacology and Toxicology Institute,^b Beijing 100850, China.

Received July 24, 1996; accepted September 6, 1996

This study describes the pharmacokinetic behaviors of taxol after intravenous administration of taxol-loaded poly(lactic-co-glycolic acid) microspheres containing isopropyl myristate (namely, Taxol-IPM-PLGA-MS) and taxol saline solution to mice. Taxol-IPM-PLGA-MS were prepared using a solvent evaporation technique. The drug content and trapping efficiency of taxol in the microspheres were 5.09% (w/w) and 98%, respectively; the average diameter of the microspheres was 30.1 μm . Scanning electron microscopy showed that Taxol-IPM-PLGA-MS were spherical with a smooth surface. After administration of the drug saline solution (3 mg taxol/kg), taxol disappeared rapidly from plasma within 4–6 h and distributed extensively in various tissues. The tissue levels and AUC_{finite} of taxol in the lung were obviously higher than those in plasma but relatively lower than those in kidneys, bile, and liver. The biodistribution of taxol after administration of Taxol-IPM-PLGA-MS (3 mg taxol/kg), on the other hand, was altered significantly from the control (taxol solution) group. No taxol was detected in plasma or bile within 3 weeks, and only very low level of taxol was detected in the kidneys or liver within 48 h. However, taxol concentrations in the lung were increased significantly with the microsphere group; the peak concentration of taxol and AUC_{finite} in the lung was three times and 500 times higher than those with the taxol solution group, respectively. It was also noticed that the taxol levels in the lung were maintained at relatively high levels ($>10 \mu\text{g/ml}$) for 3 weeks. Thus, the present study demonstrated the effective targeted delivery of taxol to the lung of mice using Taxol-IPM-PLGA-MS.

Key words taxol; poly(lactic-co-glycolic acid) microsphere; targeted delivery; pharmacokinetics; lung; mouse

Taxol is a novel antineoplastic agent isolated from the bark of the Pacific yew tree, *Taxus brevifolia*,¹⁾ with its unique antitumor mechanism of action as an inducer of tubulin assembly.²⁾ Phase I and II clinical studies have demonstrated the significant activity of taxol against a variety of solid tumors, including breast cancer, advanced ovarian carcinoma, lung cancer, head and neck carcinomas, and acute leukemias.^{3,4)} Due to the poor solubility of taxol in water and many other acceptable pharmaceutical solvents, Cremophor EL (polyoxyethylated castor oil) is used to formulate taxol in a commercial injection. However, serious hypersensitivity reactions have been reported in certain individuals since the content of Cremophor EL used in the taxol formulation is significantly higher than that in any other marketed drug.⁵⁾ Therefore, alternative dosage forms have been developed to eliminate the Cremophor vehicle by reformulating the drug in some better-tolerated vehicles, including liposomes,^{6–8)} parenteral emulsions,⁹⁾ cyclodextrin complexes,¹⁰⁾ and mixed micelles.¹¹⁾

The use of microspheres for chemo-embolization is one of the most effective approaches to enhance therapeutic efficacy of anticancer agents while reducing the systemic side effects, and some satisfactory therapeutic effects were obtained in clinical trials.^{12,13)} In our previous study,¹⁴⁾ taxol-loaded poly(lactic-co-glycolic acid) microspheres containing isopropyl myristate (IPM) as a chemical additive (namely, Taxol-IPM-PLGA-MS) were prepared and characterized *in vitro*. Approximately 70% of the initially loaded amount of taxol was released at a nearly constant rate for 3 weeks, and the microspheres showed good sphericity with an average diameter of approximately

30 μm ,¹⁴⁾ suggesting that Taxol-IPM-PLGA-MS can be used for the targeted delivery of taxol. Thus, in the present study, these microspheres were employed for targeted taxol delivery to the lung in mice; pharmacokinetic behaviors of taxol after intravenous (i.v.) administration of Taxol-IPM-PLGA-MS and taxol solution were examined, focusing particularly on the biodistribution of the drug in the targeted organ.

MATERIALS AND METHODS

Materials Taxol was a gift from Bristol-Myers Squibb Co. (Tokyo, Japan). Poly(lactic-co-glycolic acid) (average molecular weight, 10000; lactic acid/glycolic acid, 75:25), IPM, Cremophor[®] EL, phosphoric acid, dichloromethane (DCM) and acetonitrile (HPLC grade) were purchased from Nacalai Tesque Inc. (Kyoto, Japan). Gelatin and Tween 80 were of analytical grade from Wako Pure Chemical Industries, Ltd. (Osaka, Japan). *n*-Hexyl *p*-hydroxy benzoate, an internal standard of taxol for HPLC assay, was purchased from Tokyo Chemical Industry Co., Ltd. (Tokyo, Japan). Lyophilized bovine serum albumin powder (BSA) was obtained from Sigma Chemical Co. (St. Louis, Mo., U.S.A.). Double distilled water (DDW) was used throughout the experiment.

Preparation of Taxol-Loaded PLGA Microspheres Containing IPM A solvent evaporation technique¹⁵⁾ was used to prepare Taxol-IPM-PLGA-MS. PLGA (50 mg), IPM (15 mg), and taxol powder (3.5 mg) were dissolved in 1 ml of DCM. The solution, after being cooled to 4 °C, was added in a dropwise manner to 50 ml of 4% (w/v) gelatin solution stirred at 600 rpm by a magnetic stirrer

* To whom correspondence should be addressed.

and maintained at $25 \pm 1^\circ\text{C}$ in a water bath. To evaporate DCM, the stirring was continued for 1 h. Then, 25 ml of DDW was added to dilute the gelatin solution, and the microspheres were separated by centrifuging at 3000 rpm for 10 min. After removing the supernatant solution, the microspheres were collected by filtration through a cellulose nitrate membrane (pore diameter $1\mu\text{m}$, Toyo Roshi Kaisha, Ltd., Tokyo, Japan), washed three times with water, and dried at room temperature under reduced pressure. The obtained microspheres were kept in a desiccator at room temperature before use.

The taxol content in the microspheres was determined by HPLC according to the method described in our previous report.¹⁴⁾ For particle size determination, the microspheres were mounted on a slide glass and inspected under an optical microscope (IMT; Olympus, Tokyo, Japan) connected to a video camera (ICD-740; Olympus). The video signals were displayed on a computer, and the size of 300 particles was measured for each sample using an image analysis software (Image 3.0, NIH, U.S.A.).

Scanning Electron Microscopy (SEM) The shape and surface morphology of the obtained microspheres were examined with a scanning electron microscope (Hitachi S-4500, Tokyo, Japan). Microspheres were coated with gold-palladium using an ion-coater and examined under the microscope at 5.0 kV.

Animals Male ddY mice (8 weeks, 30–37 g) were obtained from Sankyo Laboratory Co., Ltd. (Toyama, Japan) and were used throughout the experiment. The mice were allowed free access to standard rodent chow and water.

Preparation of Taxol Dosages The taxol microspheres (10 mg) were dispersed in 1 ml of saline containing 0.05% (w/v) of Tween 80 just before use and vortexed for their better suspension. The taxol stock solution was prepared according to the commercial formulation of the drug. In brief, taxol was dissolved in dehydrated ethanol with an equal volume of Cremophor EL, facilitated by sonification for 20 min to obtain the taxol stock solution (6 mg/ml). The solution was kept at 4°C and used within 10 d. On the day of administration, the stock solution was brought to room temperature, diluted with saline to a final concentration of 0.5 mg/ml of taxol, and used within 20–30 min.

Pharmacokinetic Studies Two hundred μl of Taxol-IPM-PLGA-MS suspension (10 mg/ml) was administered by a single i.v. bolus injection through the jugular vein of mice ($n=4$) under light anesthesia with diethyl ether. Blood, bile, and tissues were obtained at 2, 12, 24, 48, 72, 168, 336, and 504 h after the administration of the microspheres. Blood was collected from the carotid artery in a 1.5 ml heparinized polypropylene microtube. The tubes were centrifuged immediately at 12000 rpm for 5 min; the plasma supernatant was separated and stored at -20°C until analysis. Bile was drawn from the gall bladder with a 1-ml disposable syringe to which a 26-gauge needle was attached. After the bile was weighed, 1 ml of 4% (w/v) BSA solution was applied to dilute the bile sample. The liver (0.3–0.9 g), kidneys, and lungs were dissected rapidly from the mice after exsanguination, rinsed with saline, and blotted dry. All the tissue and bile samples were weighed

and stored at -20°C until analysis. The taxol contents in plasma, bile, and tissue samples were analyzed within 2 weeks. For a control experiment, 200 μl of taxol saline solution (0.5 mg/ml) was given by an i.v. bolus injection through the jugular vein of mice ($n=4$). At 15, 30 min, 1, 2, 4, 6, 8, and 12 h after the injection, blood, bile, and tissue samples were collected, followed by the same procedure described above.

Analysis of Taxol Plasma, bile, and tissue concentrations of taxol were determined by HPLC according to the method of Mase *et al.*¹⁶⁾ with some minor modifications. Frozen samples were thawed in a water bath at 4°C . Tissue samples were homogenized at 1400 rpm in 1/15 M phosphoric acid solution using a tissue homogenizer (Ikemoto Scientific Technology Co., Ltd., Tokyo, Japan). Approximately 1.5, 4, and 5 ml of 1/15 M phosphoric acid solution were used for the homogenization of lung, kidneys, and liver samples, respectively. Then, the tissue homogenates were centrifuged at 3600 rpm for 15 min at 4°C , and the supernatants were used for taxol assay.

A solid-phase extraction (SPE) procedure was applied for sample pretreatment before HPLC analysis, employing Sep-Pak cartridge C_{18} columns (Waters Assoc., MA, U.S.A.). The SPE columns were conditioned with 5 ml of acetonitrile and then with 5 ml of DDW. Plasma samples (200–600 μl) were diluted with 2 ml of DDW; bile samples were mixed with 1 ml of DDW and loaded on the SPE columns. Immediately, 1 μg of the internal standard was applied to the columns; the columns were washed with 4 ml of DDW, and then with 4 ml of 30% (v/v) acetonitrile solution. Finally, the eluate was collected after the addition of 4 ml of acetonitrile. The eluate was evaporated to dryness under a nitrogen gas stream at 40°C in a water bath. The residue was reconstituted in 250 μl of acetonitrile: 2 mM phosphoric acid (50:50, v/v) by vortex-mixing for 15 s. Thus obtained samples were filtered through a 0.2- μm filter (GL Science, Tokyo, Japan) and the filtrates were used for taxol analysis.

For HPLC analysis, a reverse-phase column (Inertsil ODS-5; $150 \times 4.6\text{ mm i.d.}$, particle size $5\mu\text{m}$, GL Science) equipped with a μ -Bondapak C_{18} guard column ($50 \times 4\text{ mm i.d.}$, particle size $5\mu\text{m}$, Waters Assoc.) was used and the column temperature was controlled at 40°C with a column oven (CTO-6A; Shimadzu, Kyoto, Japan). The mobile phase, consisting of a mixture of acetonitrile and 2 mM phosphoric acid (50:50, v/v), was delivered at a flow rate of 1.5 ml/min with a pump (LC-6AD; Shimadzu). A 100 μl -aliquot of the samples was injected with an autoinjector (SIL-9A; Shimadzu) and column effluent was detected at 227 nm with a UV detector (SPD-6A; Shimadzu). The area of each eluted peak was integrated with an integrator (C-R6A; Shimadzu).

The taxol concentration in each sample was calculated using the ratio of the peak areas of taxol and the internal standard by comparing that ratio with a corresponding standard curve prepared in the appropriate blank samples. The calibration curve used for the quantification of taxol was linear over the range of 30–5000 ng/ml in plasma, 100–5000 ng/g in the lung, 50–3000 ng/g in the kidneys, 20–4000 ng/g in the liver, and 1–50 $\mu\text{g/g}$ in bile, with the

correlation coefficient of $r^2 > 0.995$.

Pharmacokinetic Analysis The plasma, bile, and tissue concentrations of taxol vs. time curves were characterized by a moment method implemented in a Microsoft Excel macro¹⁷⁾ to obtain model-independent pharmacokinetic parameters, *i.e.*, the area under the plasma, bile, and tissue concentration vs. time curves (AUC), mean residence time (MRT) in plasma, mean transit time (MTT) in bile and tissues, total body clearance (Cl_{tot}), the volume of distribution (V_d), and the elimination half-time ($t_{1/2}$). In order to assess the extent of tissue distribution on a concentration basis, the distribution index (namely, DI) of taxol was defined as follows:

$$DI(\%) = \frac{AUC_{finite} \text{ in each tissue or plasma}}{\text{sum of } AUC_{finite} \text{ in various tissues and plasma}} \times 100$$

Statistical Analysis Significant differences between the observed data were assessed by Student's *t*-test.

RESULTS

Size, Drug Content, and Surface Morphology of Taxol-IPM-PLGA-MS The solvent evaporation technique was used successfully to formulate the taxol-loaded microspheres. The drug content in Taxol-IPM-PLGA-MS was $5.09 \pm 0.03\%$ (w/w) (mean \pm S.D., $n=4$) and the

trapping efficiency of taxol, which is calculated as the ratio of drug weight in the produced microspheres to that used for the preparation, was approximately 98%. The average diameter of the microspheres was $30.1 \pm 11.9 \mu\text{m}$ (mean \pm S.D.; $n=300$); 93.8% of them dispersed in a range from 7 to $65 \mu\text{m}$ on the basis of particle number; the average diameter was almost the same among the three batches of the microspheres. SEM showed that the placebo PLGA microspheres (without a drug) were spherical with a smooth surface (Fig. 1a). Incorporation of 30% (w/w) IPM and 5% (w/w) taxol had no obvious influence on the shape of the microspheres except that some pores were noticed on the surface. The taxol microspheres were fairly spherical without evidence of aggregation; no taxol crystals were found on the surface (Fig. 1b).

Pharmacokinetic Analysis of Taxol after Administration of Taxol-IPM-PLGA-MS and Drug Solution The mice well tolerated the i.v. administration of Taxol-IPM-PLGA-MS at the dose of 2 mg/body, and all mice survived until the end of the experiment. The biodistribution data of taxol in plasma, bile, and tissues after i.v. administration of taxol solution and the taxol microspheres are given in Tables 1 and 2, respectively. The pharmacokinetic parameters of taxol in plasma and tissues obtained by a moment analysis are listed in Tables 3 and 4, respectively.

Taxol disappeared rapidly from plasma within 4–6 h

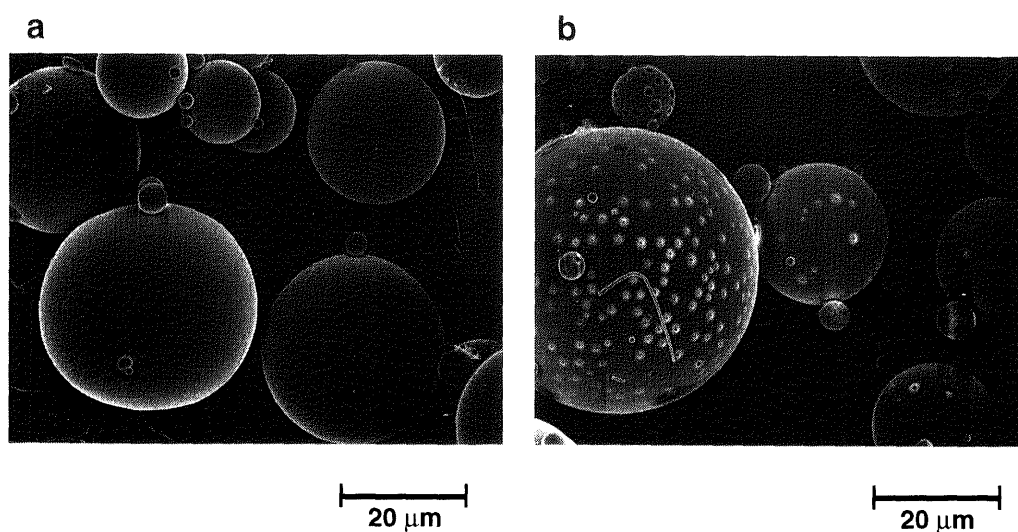


Fig. 1. Scanning Electron Micrographs Showing Surface Morphology of Placebo Poly(lactic-co-glycolic acid) Microspheres (a, $\times 500$) and Taxol-IPM-PLGA-MS (b, $\times 500$)

The loading levels of taxol and IPM were 5% (w/w) and 30% (w/w), respectively.

Table 1. Biodistribution of Taxol in Mice after i.v. Administration of Taxol Solution at the Dose of 3 mg Taxol/kg

Time	Lung ^{a)}	Liver ^{a)}	Kidney ^{a)}	Bile ^{a)}	Plasma ^{b)}
15 min	8433 \pm 644	51510 \pm 6040	16848 \pm 877	15748 \pm 6474	2890 \pm 472
30 min	5069 \pm 531	35712 \pm 4056	10024 \pm 228	14367 \pm 2181	503 \pm 25
1 h	2992 \pm 879	21361 \pm 2586	6572 \pm 1392	15514 \pm 8325	171 \pm 29
2 h	2145 \pm 477	19135 \pm 6141	5641 \pm 890	16917 \pm 7321	138 \pm 43
4 h	942 \pm 282	6685 \pm 1893	1400 \pm 368	16896 \pm 6767	27 \pm 7
6 h	539 \pm 142	6194 \pm 1010	1165 \pm 471	12412 \pm 3079	ND
8 h	147 \pm 77	2980 \pm 781	507 \pm 69	1878 \pm 703	ND
12 h	48 \pm 57	1079 \pm 408	386 \pm 73	ND	ND

Each value represents the mean \pm S.D. of four mice. a) Taxol concentration in ng/g. b) Taxol concentration in ng/ml. ND: not detected.

Table 2. Biodistribution of Taxol in Mice after i.v. Administration of Taxol-Loaded PLGA Microspheres Containing IPM at the Dose of 3 mg Taxol/kg

Time (h)	Lung ^{a)}	Liver ^{a)}	Kidney ^{a)}	Bile ^{a)}	Plasma ^{b)}
2	26169 ± 3596	436 ± 64	74 ± 25	ND	ND
12	19019 ± 5115	ND	ND	ND	ND
24	17695 ± 3013	88 ± 33	ND	ND	ND
48	11115 ± 3846	44 ± 9	ND	ND	ND
72	11857 ± 3109	ND	ND	ND	ND
168	10930 ± 4687	ND	ND	ND	ND
336	14995 ± 5165	ND	ND	ND	ND
504	11981 ± 3499	ND	ND	ND	ND

Each value represents the mean ± S.D. of four mice. ^{a)} Taxol concentration in ng/g. ^{b)} Taxol concentration in ng/ml. ND: not detected.

Table 3. Pharmacokinetic Parameters of Taxol in Plasma after i.v. Administration of Taxol Saline Solution to Mice at the Dose of 3 mg Taxol/kg^{a)}

Parameter	Taxol saline solution
$t_{1/2}$ (h)	0.97
AUC_{0-6h} (μg·h/ml)	1.20
MRT_{0-6h} (h)	0.97
V_d (ml/kg)	3010
Cl_{tot} (ml/h/kg)	2413
DI (%)	0.5

^{a)} Each parameter was calculated from the average taxol concentrations in plasma ($n=4$) at times when the mice were exsanguinated for blood sampling.

Table 4. Pharmacokinetic Parameters of Taxol in Tissues after i.v. Administration of Taxol-Loaded PLGA Microspheres Containing IPM and Taxol Saline Solution to Mice at the Dose of 3 mg Taxol/kg^{a)}

Parameter	Taxol saline solution			
	Lung	Liver	Kidneys	Bile
C_{max} (μg/ml)	8.43	51.51	16.85	16.92
$t_{1/2}$ (h)	1.65	2.26	2.16	3.44
AUC_{finite} (μg·h/ml)	12.55	104.2	27.58	103.5
MTT_{finite} (h)	2.31	2.97	2.60	3.41
DI (%)	5.0	41.8	11.1	41.6

Parameter	Taxol-IPM-PLGA-MS		
	Lung	Liver	Kidneys
C_{max} (μg/ml)	26.17	0.44	0.07
$t_{1/2}$ (h)	936	116	— ^{b)}
AUC_{finite} (μg·h/ml)	6613	3.21	0.44
MTT_{finite} (h)	254	21.5	— ^{b)}
DI (%)	99.94	0.05	0.01

^{a)} Each parameter was calculated from the average taxol concentrations in bile and tissues ($n=4$) at times when the mice were exsanguinated for sampling. ^{b)} Not applicable due to the scarcity of data.

after administration of the drug solution (Table 1). The $t_{1/2}$ and Cl_{tot} were 0.97 h and 2413 ml/h/kg, respectively, which demonstrated the rapid elimination of taxol from plasma. The V_d of taxol was 3010 ml/kg, which is obviously larger than the volume of total body water, indicating that taxol was extensively distributed in tissues. The maximum tissue level of taxol was observed in the liver, and the

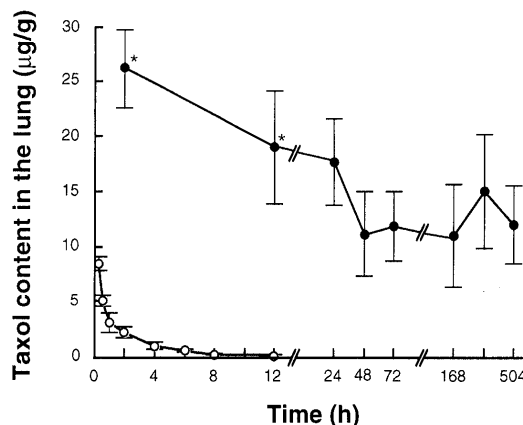


Fig. 2. Time Courses of Taxol Levels in the Lung of Mice after i.v. Administration of Taxol-IPM-PLGA-MS and Drug Solution at the Dose of 3 mg Taxol/kg

Each value and vertical bar represent the mean ± S.D. of four mice. * $p < 0.01$, significantly different from the control (taxol solution) group.

AUC_{finite} of taxol in various tissues was approximately 10–87 times higher than that in plasma. The DI value, a drug distribution index, after injection of the taxol saline solution was the highest in the liver and bile, and lower in the lung (Table 4).

The biodistribution of taxol after administration of Taxol-IPM-PLGA-MS was altered markedly from that of taxol solution, however. As shown in Table 2, no taxol peak was detected in plasma or bile samples within 3 weeks, and only a very low amount could be detected in kidneys at 2 h and in liver within 48 h. The DI values for the liver, kidney, bile, and plasma were extremely low, indicating the strongly suppressed distribution of taxol in the systemic circulation and non-targeted organs. In contrast, the peak concentration of taxol in the lung was approximately three times that in the taxol solution group; the AUC_{finite} in the lung for the microsphere group was 500 times higher than that in the taxol solution group. Furthermore, almost 100% DI in the lung demonstrated the effective targeted delivery of the drug to that organ with the microspheres.

The taxol concentration in the lung vs. time curves in the microsphere group and the drug solution group are shown in Fig. 2. There was a significant difference in taxol concentration ($p < 0.01$) between the two groups at 2 and 12 h. Taxol disappeared rapidly from the lung within 12 h after administration of the drug solution, and $t_{1/2}$ was approximately 1.6 h. However, the concentration of taxol in the lung after administration of Taxol-IPM-PLGA-MS was maintained at relatively high and constant levels ($> 10 \mu\text{g/ml}$) for 3 weeks after a progressive decline on the first 2 d. The $t_{1/2}$ of taxol in the lung was 936 h.

DISCUSSION

Some taxol-induced toxicities, such as myelosuppression, mucositis, esophagitis, and peripheral neuropathy, have been found to be related with its AUC in plasma and/or steady state plasma concentration of taxol (C_{ss}) in early clinical pharmacokinetic studies.¹⁸⁾ Therefore, the targeted delivery of taxol should be highly beneficial in

reducing its dose-limiting toxicity and enhancing the antitumor efficacy. It has been demonstrated that the targeted delivery of microspheres *in vivo* depends mainly on their particle size and route of administration.¹⁹⁾ Particles larger than 7 μm can be trapped in the capillary bed of lungs after i.v. administration. Therefore, in this study, the taxol microspheres with an average diameter of 30 μm were produced and tested for the specific delivery of taxol to the lung.

Pharmacokinetics of taxol have been studied extensively in phase I and II clinical trials^{18,20)}; however, fewer reports on its distribution in tissues have been found in either humans or animals. Some pharmacokinetic studies of taxol in animals have been performed by determining the radioactivity in plasma and tissues after i.v. administration of [^3H]taxol,²¹⁾ although the levels and changes of radioactivity with time do not represent the actual behaviors of the unchanged form of taxol because of its extensive metabolism.²²⁾ Eiseman *et al.*²³⁾ used an HPLC method to define the pharmacokinetics of taxol in plasma and tissues after i.v. administration of 22.5 mg/kg to mice and found its broad distribution in most tissues. Due to the poor sensitivity of their assay (the limit of quantitation in plasma and tissues: 0.5 and 0.8 $\mu\text{g/ml}$, respectively), however, this method may not be suitable for the pharmacokinetic study of taxol after targeted delivery using Taxol-IPM-PLGA-MS. Mase *et al.*¹⁶⁾ recently reported a simple and sensitive HPLC method for the determination of taxol in biological fluids, which was also shown to be suitable to determine its tissue distribution in experimental animals.²⁴⁾ Thus, in this study, the method of Mase *et al.*¹⁶⁾ was used to evaluate the pharmacokinetic behavior of taxol after administration of Taxol-IPM-PLGA-MS in mice.

According to the published pharmacokinetic data in clinical trials and in animal experiments, metabolism, bile excretion, and/or extensive tissue binding are believed to account for the bulk of the taxol disposition *in vivo*.^{18,25)} The drug is readily metabolized by liver and eliminated mainly through biliary secretion.²⁶⁾ Only 10% of the total clearance of taxol was accounted for by renal excretion, while 40% of that administered was recovered in bile collected for 24 h in rats as both parent compound and its metabolites.²⁷⁾ Thus, in this study, the pharmacokinetics of taxol in the liver, bile, kidney, lung, and plasma were assessed to learn the behavior of Taxol-IPM-PLGA-MS after i.v. administration, by which the microspheres can be selectively delivered to the lung due to their large size.

After administration of Taxol-IPM-PLGA-MS, the disposition profile of taxol was changed significantly from that after injection of taxol saline solution (Table 4). The drug was concentrated highly in the lung (Table 4 and Fig. 2). In vascular site-directed chemotherapy, the released drug may be extracted during the first-pass through the capillary bed of the target region, which leads to regional drug levels higher than those after conventional i.v. chemotherapy. The extent of the regional drug level escalation depends mainly on the binding affinity of the drug with a tissue.²⁸⁾ After an i.v. administration of taxol solution, taxol was eliminated rapidly from plasma and distributed extensively in various tissues, indicating its high

affinity with these tissues, possibly due to its binding to tubulin and other tissue proteins. Thus, it is not surprising that significantly higher levels of taxol in the lung were observed after i.v. administration of the microspheres than those found in plasma and other tissues. The absence of a large burst effect and the sustained release of taxol from the microspheres prepared by us¹⁴⁾ probably enhanced the first-pass distribution of the drug in the targeted organ. However, since the whole lung was extirpated to determine regional taxol levels, C_{lung} may represent not only the released drug but also the microsphere-derived drug content in the lung; moreover, the PLGA microspheres in the lung would finally be degraded and the drug in the microspheres released by that time. Therefore, C_{lung} should be viewed as the apparent drug concentration which roughly reflects the local drug residence in the organ. It was demonstrated in our previous report¹⁴⁾ that approximately 70% of the initially loaded taxol was released *in vitro* over 3 weeks at a nearly constant rate (*i.e.*, zero-order kinetics) from Taxol-IPM-PLGA-MS used in this study. Furthermore, another experiment showed that more rapid release of taxol from the microspheres *in vivo* occurred due to the faster degradation of the microsphere matrix (manuscript in preparation), which aids diffusion of the drug out of the matrix.^{29,30)} Thus, the relatively high and constant taxol level in the lung after administration of Taxol-IPM-PLGA-MS may be mainly attributable to the drug released from the microspheres. So far, it has been very difficult to separate the microsphere-derived drug content from the tissue-derived drug content in a quantitative manner.

In conclusion, Taxol-IPM-PLGA-MS were demonstrated to be efficiently delivered to the lung of mice with a long residence time, while the systemic exposure of non-targeted organs to taxol was significantly reduced. It is thus suggested that Taxol-IPM-PLGA-MS will enhance the anticancer efficacy in cancer chemotherapy while reducing the systemic toxicity. Further investigation should be performed to study the antitumor effect of Taxol-IPM-PLGA-MS using animal tumor models.

Acknowledgment One of the authors (Y.M.W.) wishes to thank the Nagai Memorial Foundation for their financial support.

REFERENCES

- 1) Wani M. C., Taylor H. L., Wall M. E., Coggon P., McPhail A. T., *J. Am. Chem. Soc.*, **93**, 2325—2327 (1971).
- 2) Lopes N. M., Adams E. G., Pitts T. W., Bhuyan B. K., *Cancer Chemother. Pharmacol.*, **32**, 235—242 (1993).
- 3) Rowinsky E. K., Cazenave L. A., Donehower R. C., *J. Natl. Cancer Inst.*, **82**, 1247—1259 (1990).
- 4) Donehower R. C., Rowinsky E. K., Grochow L. B., Longnecker S. M., Ettinger D. S., *Cancer. Treat. Rep.*, **71**, 1171—1177 (1987).
- 5) Weiss R. B., Donehower R. C., Wiernik P. H., Ohnuma T., Gralla R. J., Trump D. L., Baker J. R., VanEcho D. A., VonHoff D. D., Leyland-Jones B., *J. Clin. Oncol.*, **8**, 1263—1268 (1990).
- 6) Sharma A., Mayhew E., Straubinger R. M., *Cancer Res.*, **53**, 5877—5881 (1993).
- 7) Sharma A., Straubinger R. M., *Pharm. Res.*, **6**, 889—895 (1994).
- 8) Straubinger R. M., Sharma A., Murray M., Mayhew E., *J. Natl. Cancer Inst. Monogr.*, **15**, 69—78 (1993).
- 9) Tarr B. D., Sambandan T. G., Yalkowsky S. H., *Pharm. Res.*, **4**,

- 162—165 (1987).
- 10) Sharma U. S., Balasubramanian S. V., Straubinger R. M., *J. Pharm. Sci.*, **84**, 1223—1230 (1995).
- 11) Alkan-Onyuksel H., Ramakrishnan S., Chai H.-B., Pezzuto J. M., *Pharm. Res.*, **11**, 206—212 (1994).
- 12) Ichihara T., Sakamoto K., Mori K., Akagi M., *Cancer Res.*, **49**, 4357—4362 (1989).
- 13) Wang J., Li L. S., Feng Y. L., Yao H. M., Wang X. H., *Chin. Med. J.*, **106**, 441—445 (1993).
- 14) Wang Y. M., Sato H., Adachi I., Horikoshi I., *Chem. Pharm. Bull.*, **44**, 1935—1940 (1996).
- 15) Juni K., Ogata J., Nakano M., Ichihara T., Mori K., Akagi M., *Chem. Pharm. Bull.*, **33**, 313—318 (1985).
- 16) Mase H., Hiraoka M., Suzuki A., Nakanomyo H., *Yakugaku Zasshi*, **114**, 351—355 (1994).
- 17) Sato H., Sato S., Wang Y. M., Horikoshi I., *Comp. Methods Prog. Biomed.*, **50**, 43—52 (1996).
- 18) Rowinsky E. K., Wright M., Monsarrat B., Donehower R. C., *Annals. Oncol.*, **5** (suppl. 6), S7—S16 (1994).
- 19) Gupta P. K., Hung C. T., *J. Microencapsulation*, **4**, 427—462 (1989).
- 20) Wiernik P. H., Schwartz E. L., Strauman J. J., Dutcher J. P., Lipton R. B., Paietta E., *Cancer Res.*, **47**, 2486—2493 (1987).
- 21) Klecker R. W., Jamis-Dow C. A., Egorin M. J., Erkmen K., Parker R. J., Stevens R., Collins J. M., *Drug Metab. Dispos.*, **22**, 254—258 (1994).
- 22) Walle T., Kumar G. N., McMillan J. M., Thornburg K. R., Walle U. K., *Biochem. Pharmacol.*, **46**, 1661—1664 (1993).
- 23) Eiseman J. L., Eddington N. D., Leslie J., MacAuley C., Sentz D. L., Zuhowski M., Kujawa J. M., Young D., Egorin M. J., *Cancer Chemother. Pharmacol.*, **34**, 465—471 (1994).
- 24) Fujita H., Okamoto M., Takao A., Mase H., Kojima H., *Jpn. J. Cancer Chemother.*, **21**, 659—664 (1994).
- 25) Rowinsky E. K., Wright M., Monsarrat B., Lesser G. J., Donehower R. C., *Cancer Surveys*, **17**, 283—304 (1993).
- 26) Monsarrat B., Alvinerie P., Wright M., Dubois J., Guéritte-Voegelein F., Guénard D., Donehower R. C., Rowinsky E. K., *J. Natl. Cancer Inst. Monogr.*, **15**, 39—46 (1993).
- 27) Monsarrat B., Mariel E., Cros S., Garès M., Guénard D., Guéritte-Voegelein F., Wright M., *Drug Metab. Dispos.*, **18**, 895—901 (1990).
- 28) Stephens F. O., *Reg. Cancer Treat.*, **1**, 4—10 (1988).
- 29) Heya T., Okada H., Ogawa Y., Toguchi H., *J. Pharm. Sci.*, **83**, 636—640 (1994).
- 30) Kamei S., Inoue Y., Okada H., Yamada M., Ogawa Y., Toguchi H., *Biomaterials*, **13**, 953—958 (1992).